Dynamic memory in a microfluidic system of droplets traveling through a simple network of microchannels†

Olgierd Cybulski* and Piotr Garstecki*

Received 1st July 2009, Accepted 1st October 2009
First published as an Advance Article on the web 1st December 2009
DOI: 10.1039/b912988j

The flow of droplets through the simplest microfluidic network—a set of two parallel channels with a common inlet and a common outlet—exhibits a rich variety of dynamic behaviors parametrized by the frequency of feeding of droplets into the system and by the asymmetry of the arms of the microfluidic loop. Finite ranges of these two parameters form islands of regular (cyclic) behaviors of a well defined period that can be estimated *via* simple theoretical arguments. These islands are separated by regions of behaviors that are either irregular or cyclic with a very long periodicity. Interestingly, theoretical arguments and numerical simulations show that within the islands of regular behaviors the state of the system can be degenerate: there can exist a number of distinct sequences of trajectories of droplets, each stable and—in the absence of disturbances—continuing *ad infinitum*. The system can be switched between these cyclic trajectories with a single stimulus.

1 Introduction

We demonstrate numerically and confirm experimentally the existence of dynamic memory in a system of droplets traveling through a simple microfluidic device: a single channel split into two that subsequently recombine again to a single outlet. The operation of the system is parametrized by the geometry of the channels, the pressure drop along the system, and the frequency and added resistance of the droplets introduced into the flow. We show that there are finite (and wide) regions in the parameter space for which the system operates periodically. Within each of these regions there is a finite number of stable cyclic sequences of the trajectories of the droplets. Each of these sequences can repeat *ad infinitum* unless the system is switched by an external stimulus (*i.e.* by application of a transient perturbation of the parameters) into a different sequence. Our observations provide an example of a microfluidic system that exhibits memory and an example of a detailed understanding of *digital* (droplet) flows in topologically non-trivial networks.

The interest in flow of droplets through microfluidic networks stems from the challenge of building digital chip laboratories capable to perform complex chemical protocols and screens. Since the introduction of immiscible flows in microfluidic systems[1] the ability to form monodisperse droplets[2,3] and bubbles[4,5] has generated an immense interest in the idea of utilizing droplets as microscale reaction beakers[6] that can be formed at high frequencies (*e.g.* 1 kHz) and with high reproducibility.[7,8] Several protocols of chemical syntheses and analyzes have been reported to date.[6,9] Most of these demonstrations, however, utilize simplistic, linear systems in which the droplets travel through a network comprised of essentially one main channel supplemented only with a number of inlets, and possibly more than one outlet for sorting.

Thus the current state of art falls short of the outstanding vision (and challenge) of designing versatile chips for *e.g.* combinatorial analysis or synthesis, with different conditions of reaction or incubation (times, temperature, exposition to light, *etc.*) probed in controlled, sequential or parallel protocols, and with arbitrarily designed conditions for sorting and retrieving the products. Reaching this goal demands construction of a microfluidic network with several inlets for a large number of reagents to be screened against each other and a topologically non-trivial network of channels and outlets. Although there are clever solutions[10] that might greatly facilitate the task, we are far from accomplishing it because of the complexity of the dynamics of flow of discrete *resistors* through networks.[11–13]

1.1 Complexity of the flow of droplets through microfluidic networks

Droplets traveling through microfluidic ducts increase the resistance to flow of the capillary that they occupy.[14,15] In microfluidic networks this effect is supplemented with (i) long range interactions between the droplets mediated *via* the pressure field, and (ii) delays in the relaxation of the content of any channel associated with the time of travel in that duct. In consequence, the trajectory of any droplet through the system may depend on the details of the trajectories of a number of preceding droplets. These effects lead to *e.g.* periodic and irregular sequences of trajectories of droplets,[11] dependence on the history of the system[13] and form the basis of demonstrations of encrypting/decrypting strategies[12] or of construction of microfluidic logic gates.[16]

The experiments by Fuerstman *et al.*[12] demonstrated a striking feature of the 'digital' flows through microfluidic networks: in spite of the nonlinear elements of the dynamics that provide for elementary signal processing[12] or logic operations,[16] the linearity of the underlying equations of flow (at low or moderate Reynolds

Institute of Physical Chemistry, Polish Academy of Sciences, Kasprzaka 44/52, 01-224 Warsaw, Poland. E-mail: olgierd@ryba.ichf.edu.pl; garst@ichf.edu.pl

† Electronic supplementary information (ESI) available: Videos that document all ten possible periodic sequences of trajectories of eight droplets in a microfluidic loop, exactly as predicted by the theory. See DOI: 10.1039/b912988j

numbers) provide for robustness of the dynamics against small perturbations.[12] These demonstrations offered two promises: (i) that elementary but non-trivial protocols can be accomplished even in passive—that is, lacking detailed external control—systems, and (ii) that such protocols can be realized in practice without amplification of the inevitable experimental noise into chaotic or erratic dynamics.

Although microfluidic operations on droplets are not intended to conquer the computational market, there is an important applied consequence of the above observations. Even a small number of sequential elementary operations (leading to selecting of a particular channel, splitting or merging of droplets) can provide for a vast number of combinations of reagents and conditions of reactions. Such carefully designed protocols of droplet flows can open the way to miniaturizing a fully functional chemical laboratory onto a microfluidic chip. Since the techniques for formation,[17,18] splitting,[19,20] merging[20–22] and guiding[10,22,23] of droplets are constantly developed, the crucial and lacking step in reaching this goal is understanding of the flow of droplets through networks.

Here we show the application of a numerical scheme[13,24] to a detailed mapping of the possible sequences of trajectories of droplets in the simplest microfluidic network – a simple loop. In the following sections we discuss the model, introduce the basic phenomenology on the simple example of a *synchronized* state in a symmetric loop and further extend the description to a general case of a loop of arbitrary dimensions with examples of memory in the system. Finally we describe the experiments that confirm the numerical predictions.

2 The model

We built the model on the analogy between electric and hydraulic systems operating at low Reynolds numbers. We use Kirchhoff's circuit laws to calculate node pressures and flow through each channel of the network. The distribution of resistance in the network comprises two contributions: one (static) from the resistance of the channels, and the second (dynamic) from the presence of droplets in the channels. Once the geometry and topology of the system is set, we apply a constant flux of identical droplets (introduced at a frequency f) into the inlet of the system together with the continuous flow of the matrix fluid.

2.1 Basic notions and assumptions in the model

We model the channels as one-dimensional wires. Droplets are represented by nondimensional points which move along these wires with velocity $V = Q/A$, where Q is a volumetric flow rate of the continuous fluid in a given channel and A is a constant having the dimension of surface area. If A is the cross-section of the channel, V becomes the superficial (average) speed of flow; other values of A may be used for modeling droplets which move faster or slower than the continuous fluid. The exact value of A does not introduce qualitative changes into the results produced by the model - it only sets the time scale. A more important set of assumptions that we adopt here is that the ratio of the speed of the droplets to the superficial speed of flow does not depend neither on their size (charge of resistance) nor on the distance between the droplets. While the first assumption has experimental support for liquid and gaseous plugs,[15,25] second is valid only for distances between the droplets that are large enough to eliminate hydrodynamic interactions between them. This condition is met in our experiments.

If the pressure drop in a channel is p, we calculate the speed of flow (V) using Ohm's law:

$$V = \frac{Q}{A} = \frac{p}{AR} = \frac{p}{A(R_0 + nr)} \quad (1)$$

where R is the total hydrodynamic resistance comprising the constant resistance of the channel, R_0, and the sum of resistances carried by the droplets (nr) for n identical droplets each carrying the same resistance r. As long as all channels have the same, constant, cross-section the constant part of resistance, R_0, is proportional to the length of a channel, L. The additional resistance r introduced by a droplet in the channel may be expressed as an increase of the length of the channel by $\delta L_{\mathrm{drop}} = (r/R_0)L$. This quantity is unrelated to the physical length of droplets in real systems.

The flow of liquid through the system is driven by the pressure difference between the inlet and the outlet and may be controlled in two different ways: by setting this pressure difference to a constant value or by fixing the total volumetric flow with pressure being dependent on the number and position of droplets along the network. All the other (internal) pressures and speeds of flow in each of the channels are dependant variables. Step changes of these quantities take place when: (i) a new droplet enters the system at the inlet (ii) a droplet leaves the system at the outlet (iii) any droplet traverses from one channel to another through an internal node. In the last case, when a droplet arrives at an internal junction, the droplet enters the channel with the largest momentary inflow (calculated before the act of the droplet entering the channel).

2.2 Numerical details

Introduction of a new droplet into the system, a droplet reaching an internal node, or reaching the outlet are three types of events that change the content of the channels. Between these events all droplets are carried along their channels at constant speeds. The simulation cycle consists of the following steps: (i) for a given configuration of droplets, calculate the resistance in all channels, R_i (where i denotes i-th channel). (ii) Given the values of resistance and external pressure, calculate internal pressures, volumetric flow rates (Q_i) and linear velocities (V_i) in the channels. For a fixed topology of the network this calculation may be performed by custom subroutines, however, an efficient and convenient solution to the problem is to use external SPICE-based libraries such as GnuCap[24,26] which facilitate simulations of complicated networks and provides efficient algorithms for nonlinear extensions of the model: *e.g.* a dependence of resistance carried by droplets on their speed of flow (non-Ohmic case). (iii) Given the velocities, find the interval Δt^* until the next event. (iv) Advance the positions of the droplets by $\Delta x_i = V_i \Delta t^*$. If a droplet arrives at a junction, translate it to the starting position in a new channel, selected by the larger Q_i. The resulting configuration is then used in the next cycle.

The described simulation method is exact; errors are only due to floating-point arithmetics. All the velocities, flow rates and

internal pressures are piecewise constant, whereas positions of droplets in channels are piecewise linear functions of time.

3 Stationary state of a single channel

Let us first consider the stationary state of a single channel, in which the quantities p, R, n, Q, V are constant in time; not only in the sense of average values, but literally constant. For $n > 0$, this is possible if and only if the event of a droplet leaving the channel is synchronized with an introduction of a new droplet at the inlet. We call such a dynamic condition a synchronized stationary state (see Fig. 1.a). If the droplets enter the channel at frequency f, the distance between two subsequent droplets in the channel may be expressed as V/f. In the synchronized state the droplets must be equally spaced along the channel, with the interval equal to L/n. Equating these two expressions yields:

$$V = \frac{Lf}{n} \tag{2}$$

V must also satisfy the basic assumptions given in sect.2.1. Combining eqn (2) and eqn (1) we obtain the frequency of the synchronized stationary state with n droplets in the channel:

$$f = \frac{p\ n}{A\ L\ (R_0 + n\,r)} \tag{3}$$

or, alternatively n as a function of f:

$$n = \frac{(R_0/r)\ (f/f_\infty)}{1 - (f/f_\infty)} \quad \text{where :} \quad f_\infty = \frac{p}{ALr} \tag{4}$$

The parameter f_∞ may be interpreted as a critical frequency of dripping: when $f \to f_\infty$, the number of droplets in the channel goes to infinity. Such an interpretation is not physical: in a real system for any finite size of the droplets there is a maximum number that can be contained in the channel. Nonetheless, we will show that f_∞ is a usefull parameter of the model also in the physical range of frequencies, *i.e.* for finite n. In the following we use f_∞ to nondimensionalize the frequency of feeding of the droplets into the system (f/f_∞). Similarly, we use n_0, defined as $n_0 = R_0/r$ to scale n. The dependence of such renormalized number of droplets, n/n_0, on the dimensionless frequency, f/f_∞, is shown in Fig. 1.b. Integer values of n correspond to the synchronized states.

Arbitrary values of f in eqn (4) lead to non-integer values of n. These stationary states are not synchronous: the number of droplets $n(t)$ oscillates between two integers nearest to n given by eqn (4), so that the average value of $n(t)$ is very close to n.

4 Flow of droplets through a symmetric loop

4.1 Synchronized states

Before we describe the general behavior of droplets flowing through an arbitrary loop, it is useful to consider the simplest case that illustrates the degeneracy of the periodic trajectories of droplets. Just as we defined a synchronized state for a single channel, we can construct a similar condition for a symmetric loop: a system of two parallel channels of equal length ($L_a = L_b$) and initial resistance ($R_{0a} = R_{0b}$), with a common inlet and a common outlet. As illustrated in Fig. 2 in this configuration we can imagine that the event of any droplet leaving the system is synchronized with the event of a new droplet introduced into the loop. Obviously, in the 'stationary' state consisting of $n = n_a + n_b$ droplets in the whole loop, the number of droplets in each of the

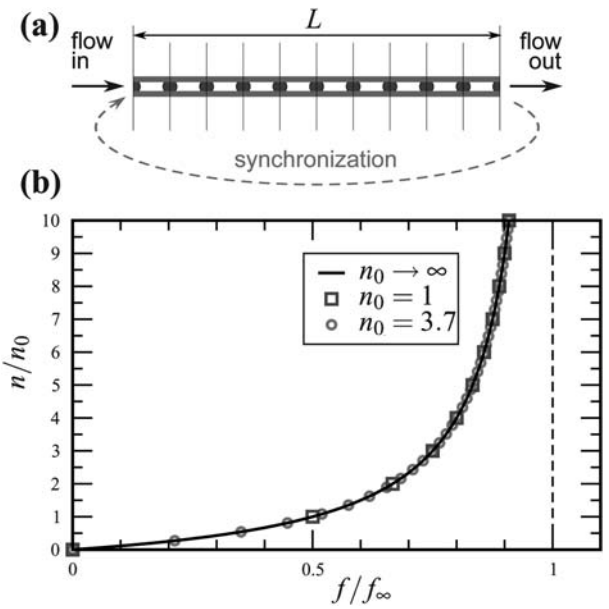

Fig. 1 (a) Synchronized stationary state of a single channel at a constant frequency of dripping: a new droplet enters the channel at the same time as the last droplet exits. The arrow pointing from the outlet to the inlet does not correspond to the direction of flow. It is meant to indicate synchronization of the events of a droplet leaving the channel and a (different) droplet entering it. (b) The number of droplets in a synchronized stationary state of a single channel as a function of the frequency of dripping for three different ratios of the resistance of the channel to the added resistance of the droplet $n_0 = R_0/r$. When $f \to f_\infty$, the number of droplets becomes infinitely large.

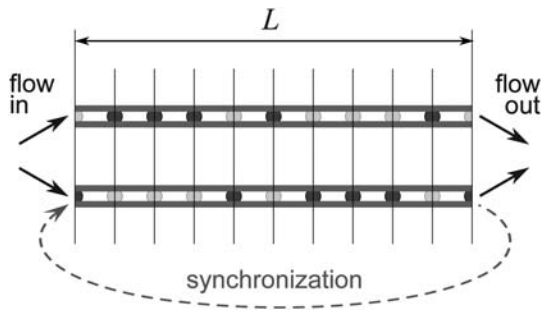

Fig. 2 A schematic representation of the synchronized state of symmetric loop. For the sake of the discussion of the combinatorial composition of the periodic patterns of trajectories we drew the arms of the loop as straight and parallel channels. It is important to remember that these channels share a common inlet and a common outlet. At synchronization frequencies the event of a droplet leaving the loop is synchronized with the event of a (new) droplet entering one of the two arms. The numbers of droplets, resistances and velocities in both channels are equal and constant in time. The vertical lines are used to derive the number of possible distributions of droplets in the synchronized state of a symmetric loop. Please consult sect.4.1 for a detailed explanation.

two arms must be equal, *i.e.* $n_a = n_b = n/2$. Consequently, when a droplet leaves one of the channels, a new droplet must enter the same channel. This is possible only for a discrete set of frequencies (*i.e. synchronization frequencies*). Similarly to eqn (3), such frequencies must be equal to:

$$f_{\text{sync}} = \frac{n\, f_{\infty\,\text{eff}}}{n + 4\, R_{0\text{eff}}/r} \tag{5}$$

where $f_{\infty\ \text{eff}} = 2f_{\infty\ a} = 2f_{\infty\ b}$, $R_{0\ \text{eff}} = R_{0a}/2 = R_{0b}/2$ (see explanation below eqn (6)) and n must be an even integer number.

4.2 Degeneracy of periodic sequences

The condition of synchronization, imposed on f_{sync} and n by eqn (5), does not determine the *distribution* of the droplets within each of the two channels. In fact, for any number $n_a = n_b = n/2$ of droplets in each of the channels there exist a class of possible distributions that yield the synchronized state. In order to construct these distributions, we divide the length of the arms, $L = L_a = L_b$, into sections of length L/n: in each channel there are n positions that must be occupied by $n/2$ droplets. This can be done in $|\Omega_{\text{distr}}| = n!/[(n/2)!]^2$ ways, with the distribution in the second channel being always the negative reflection of the distribution in the first channel (see Fig. 2). Any of such prepared distributions will be repeated *ad infinitum*. Each of the momentary distributions of droplets in the two channels corresponds to a well defined *sequence* of left/right (L/R) choices of droplets entering the loop. The period N of these cyclic sequences is n or less, *e.g.* $n/2$, $n/3$, *etc.* for super-harmonics (*e.g.* for $n = 6$ the sequence RRLLRL has a period $N = n = 6$ whereas RLRLRL has $N = n/3 = 2$).

The number of essentially different *sequences*, $|\Omega_{\text{seq}}|$, is less than the number of possible distributions $|\Omega_{\text{distr}}|$ due to the cyclic equivalence; *e.g.* for $n = 6$ there is $|\Omega_{\text{seq}}| = 4$ different sequences and $|\Omega_{\text{distr}}| = 20$ distributions, which can be grouped as 6 + 6 + 6 + 2 (six cyclic shifts of LLLRRR, LLRLRR, LLRRLR each and two cyclic shifts of LRLRLR). One way of unequivocal choice of the sequence from the cyclically shifted class is to choose the first one from the list sorted in ascending lexicographic order.

4.3 Periodicity in non-synchronized states of a symmetric loop

Interestingly, the condition of synchronization is not necessary for a sequence of the trajectories of the droplets to be periodic. Further, a sequence of particular period N (number of droplets per cycle) and with particular sequence (L/R) observed at f_{sync} can be stable also for $f \neq f_{\text{sync}}$. In Fig. 3a we show the period of the L/R sequences as a function of the frequency at which the droplets are introduced into the symmetric loop. The synchronization frequencies are marked by circles. As one can see there are finite ranges of f within which the sequences are periodic with period corresponding to the average number of droplets in the loop (or lower, if the super-harmonics are possible). For these bands (we call them *regular* bands) the value of the appropriate f_{sync} plays the role of the upper limit of frequency; sequences with the period corresponding to f_{sync} are encountered for $f \leq f_{\text{sync}}$.

The regular bands of f are interlaced by irregular bands, where the (L/R) sequence is aperiodic or periodic with a very large period. The difference between *regular* and *irregular* behavior

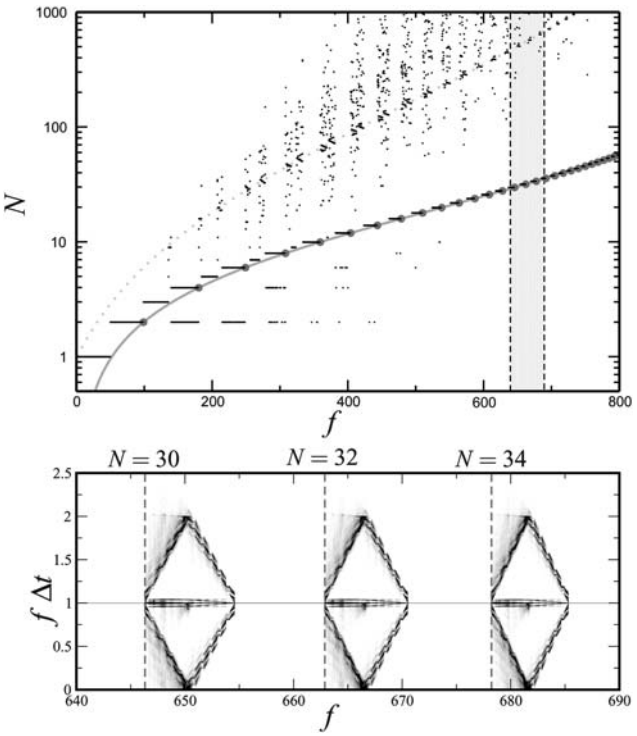

Fig. 3 Effect of the frequency f of dripping on the period of cyclic sequences and intervals between droplets exiting the symmetric loop with $L_a = L_b = 2$ mm, for $\delta L_{\text{drop}} = 0.2$ mm and $f_{\infty\ \text{eff}} = 1077.2$ Hz. (a) Number of droplets (N) forming a periodical pattern (if present), as a function of f. Circles correspond to the synchronized stationary states described in sect.4.1. Solid curve (light color) indicates theoretically calculated number of droplets in the system, n_{theo} (see eqn (6)). As a puzzle to an interested reader we also plotted the dotted curve given by $(n_{\text{theo}} + 1)(n_{\text{theo}} + 2)/2$. We observed in all of similar plots a congestion of points along this curve. (b) Normalized time intervals between consecutive droplets that leave the loop as a function of f – for a highlighted range of f in the plot (a) (the whole range of f is included in ESI). Three local values of f_{sync} are marked by the vertical dashed lines (signed by corresponding cycle length, N). In a *regular band* (below f_{sync}) there is only one interval: droplets exit the loop at the same time intervals as they enter at the inlet (regardless of what periodic sequence is actually repeated). In an *irregular band* (above f_{sync}) many different time intervals are observed, and the set of possible intervals may depend on the particular trajectory (*i.e.* on the history of the system).

exhibits not only in the period of the cyclic (L/R) sequence but also in various aspects of dynamics. Fig. 3b shows the normalized (multiplied by f) intervals of time between droplets exiting the loop, as a function of the frequency of feeding f. The range of f shown in Fig. 3b covers four regular bands divided by three irregular bands. Although the number of various sequences, $|\Omega_{\text{seq}}|$, in these regular bands is of the order of 10^6, all the sequences preserve the same output intervals (equal to the input intervals $1/f$). This behavior disappears in the irregular bands: there are many possible intervals, some of them lie in areas visited more frequently, some are isolated or prohibited, some are reached only by particular trajectories.

The fact that synchronization frequencies form the *upper* limit of the regular bands can be explained by the following heuristic argument. If we imagine the synchronized state (Fig. 2) and

slightly decrease the frequency of feeding, the spacing between the droplets will slightly increase. As a result, the event of a droplet exiting the loop will precede the event of a new droplet arriving at the inlet, and the order of L/R choices will remain unchanged. In contrast, if we increase f slightly above f_{sync}, the event of a new droplet arriving at the inlet will precede the event of a droplet exiting the loop and the sequence of choices will change.

5 Arbitrary loop

In the following sections we generalize our observations of the regular cycles to the loops of arbitrary lengths of the arms.

5.1 Expected number of droplets

Before we discuss the map of cyclic dynamics of an arbitrary loop we estimate the average number of droplets in a system of two channels of length L_a and L_b connected in parallel between common inlet and outlet. If $L_a \neq L_b$ the droplets flowing into the junction will all go into the channel characterized by the lower resistance up to a point (provided that the flux of droplets is sufficiently high) at which the resistances of the two arms will be equal modulo the resistance of a single droplet. Further increase of the flux of droplets will sustain this balance – by virtue of the assumption that every droplet flows into the arm characterized by the higher inflow (lower resistance). Thus for asymmetric loops the number of droplets (n_a, n_b) in each of the channels may be different. In order to estimate the total (integer) number $n = n_a + n_b$ of droplets in the loop as a function of the resistance of the single droplet (r) and the frequency at which they are fed into the loop (f) we use an equation that assumes a perfect balance of the resistance of the two arms and yields n_{theo}, a non-integer approximation of n:

$$n_{\mathrm{theo}}(f) = \frac{4\,R_{0\,\mathrm{eff}}}{r}\,\frac{f_{\infty\,\mathrm{eff}}}{f_{\infty\,\mathrm{eff}} - f} - \frac{R_{0a} + R_{0b}}{r} \qquad (6)$$

where the effective parameters:

$$f_{\infty\ \mathrm{eff}} = \frac{p}{A\,L_{\mathrm{eff}}\,r} = f_{\infty a} + f_{\infty b}$$

and:

$$R_{0\ \mathrm{eff}} = \frac{R_{0a}\,R_{0b}}{R_{0a} + R_{0b}}, \quad L_{\mathrm{eff}} = \frac{L_a\,L_b}{L_a + L_b}$$

represent the values of a single-channel equivalent circuit of the parallel connection of channels a and b. In Fig. 4a we show the variation of n_{theo} with the lengths of the two arms L_a and L_b and with the frequency of feeding of droplets (of resistance r corresponding to an equivalent length of the channel $\delta L_{\mathrm{drop}} = 0.2$ mm). The subsequent zones of $n - 1 < n_{\mathrm{theo}} < n$ are colored and designated by subsequent integer values of n.

5.2 Periodic dynamics

In Fig. 4b we demonstrate the results of numerical simulations of loops with a varied length of one of the channels (the other arm is fixed to a length of 2 mm) and for a wide range of frequencies of feeding of the droplets into the system. As we change the ratio of the lengths of the two arms, the intervals of the frequency for

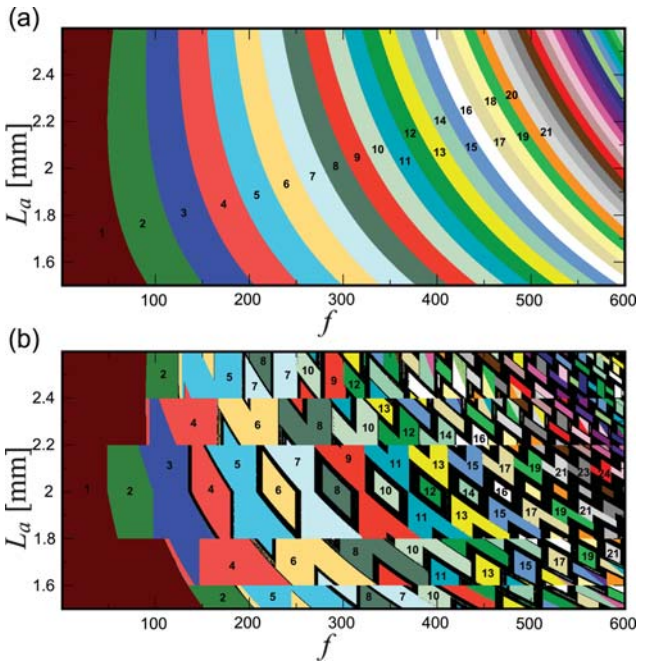

Fig. 4 Expected number of droplets in the system (a) and the number of droplets forming a regular, periodical pattern (b), as a function of parameters: f (X-axis) and L_a (Y-axis) when the remaining parameters are constant ($L_b = 2$ mm, $\delta L_{\mathrm{drop}} = 0.2$ mm). The numbers and collored fields on the map (a) give the next larger integer to n_{theo} calculated from eqn (6). Colored fields on (b) correspond to regular, periodical patterns formed by marked number of droplets (the pattern repeats itself after time N/f; super-harmonics, that may occur for some points, are ignored). Black fields correspond to aperiodic or irregular behavior (or patterns with periods much longer than number of droplets occupying the loop).

which we observe regular cyclic dynamics of the system change. In the space spanned by the frequency and the asymmetry of the arms (Fig. 4.b) the regions of regular dynamics form rhomboidal shapes separated by regions of irregular (or characterized by much longer periodicity) behavior of the system. We observe that there is a coincidence of the periodicity of the regular regions with the 'theoretical' or averaged number of droplets in the loop (please compare both maps from Fig. 4) but the relation between the two maps is nontrivial.

5.3 Dynamic memory in an arbitrary loop

An example of a set of cyclic sequences from a "regular" region is shown in Fig. 5. The parameters correspond to the point ($f = 250$ Hz, $L_a = 2.1$ μm) in Fig. 4.b, *i.e.* to one of regular regions with period $N = 7$, whereas the theoretical number of droplets in the loop is estimated from eqn (6) to $n_{\mathrm{theo}} \approx 6.38$ (Fig. 4.a) and the real average value (from integration of $n(t)$ over a full period) is $\bar{n} \approx 6.41$. In Fig. 5 we show the number of droplets in the channel a ("right" channel), changing between 2 and 3, and in b ("left" channel), changing between 3 and 4, for each of the five observed sequences. The results shown in Fig. 5 were obtained by starting the simulation with the same parameters for a large number of different initial conditions. These five sequences form a complete list of the temporal patterns we have found. The same number of possible sequences may be obtained from combinatorial

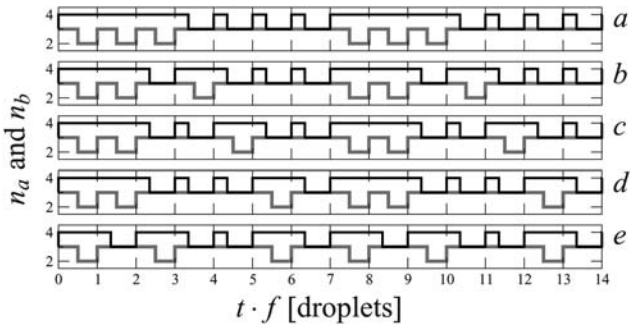

Fig. 5 Number of droplets in the right channel (n_a, values between 2 and 3) and left channel (n_b, between 3 and 4) as a function of time. The loop has arms of length 2 mm (left channel) and 2.1 mm (right channel) and the droplet equivalent length is 0.2 mm, the parameters correspond to the point ($f = 250$ Hz, $L_a = 2.1$ mm) in Fig. 4. Shown are all five patterns available for this point of parameter space: RRRLLLL (*a*), RRLRLLL (*b*), RRLLRLL (*c*), RRLLLRL (*d*), RLRLRLL (*e*).

counting of all possible permutations of three R-s and four L-s and eliminating cyclic shifts:

$$|\Omega_{\text{seq}}| = \frac{N!}{N\ N_L!\ N_R!} \tag{7}$$

For $N = N_L + N_R = 3 + 4 = 7$ there is $|\Omega_{\text{seq}}| = 5$. The N in the denominator eliminates $N - 1$ redundant cyclic shifts.

As we checked in the simulations, and as we later show experimentally, these patterns may be switched from one to another by transient disturbances, *e.g.* temporary jumps of f, p or r. As long as the parameters remain unchanged, the pattern is repeated cyclically - we call this *memory* since the pattern once introduced is memorized *ad infinitum*.

5.4 Availability of patterns

Although in our simulations we were usually able to obtain all the sequences predicted by combinatorial arguments, two interesting questions arise: (i) Whether at *any* point in the parameter space (f, L_a/L_b) that lies within a regular region, *all* the patterns expected from combinatorial considerations can be observed in simulation or experiment? (ii) Is it possible to reach a given pattern from another pattern during the continuous evolution of the system subjected to varying f, p and r? The latter question is particularly important in experiment, where it is impossible (at least with our current capabilities) to start the system from a deliberately prepared distribution of droplets. When we tested a large number of simulations with different initial conditions (*e.g.* 10^4 runs) for a fixed pair of (f, L_a/L_b) we observed that the frequency of occurence of particular sequences varies from sequence to sequence, and some temporal patterns are not exhibited at all. Similarly, introduction of transient changes in pressure or frequency of emission of droplets caused the system to switch from one pattern to another but some patterns could not be reached. We conjecture that in the space of all possible initial configurations of droplets the different patterns may have different measures of their basins of attraction. It is plausible that the basins of attraction of some patterns are of measure zero, yielding some patterns to be unreachable at all. For example, in the upper stripe of the map in Fig. 4.b there are two areas with period $N = 7$. In each of these two regions there are two droplets in the right channel (two R-s) and five droplets in the left channel (five L-s). From combinatorics, there should be three patterns: RRLLLLL, RLRLLLL and RLLRLLL, and in simulations we do observe all these three patterns in some points (*e.g.* for $L_a = 2.5$ and $f = 200$ or 230 Hz), yet – for the same $L_a = 2.5$ – we never observe the pattern RLLRLLL for $f \leq 198$, nor found RRLLLLL for $f \geq 232$.

5.5 The role of the added resistance of a single droplet

All the examples presented above correspond to simulations with one particular value of the added resistance r of a single droplet: equal to the resistance of the channel of length $\delta L_{\text{drop}} = 200$ μm. In general, changing this value does not introduce qualitative changes in the dynamics of the system. In Fig. 6 we show the periodicity and the diagram of the intervals between droplets exiting the loop obtained in simulations of an asymmetric loop (with $L_a = 2.1$, $L_b = 2$ mm) with the value of r twice bigger ($\delta L_{\text{drop}} = 400$ μm) than in all previous simulations. Differences between these results and the ones obtained for r corresponding to ($\delta L_{\text{drop}} = 200$ μm) for a symmetric loop (Fig. 3) are only quantitative; the general features of the behavior of the system remain unchanged.

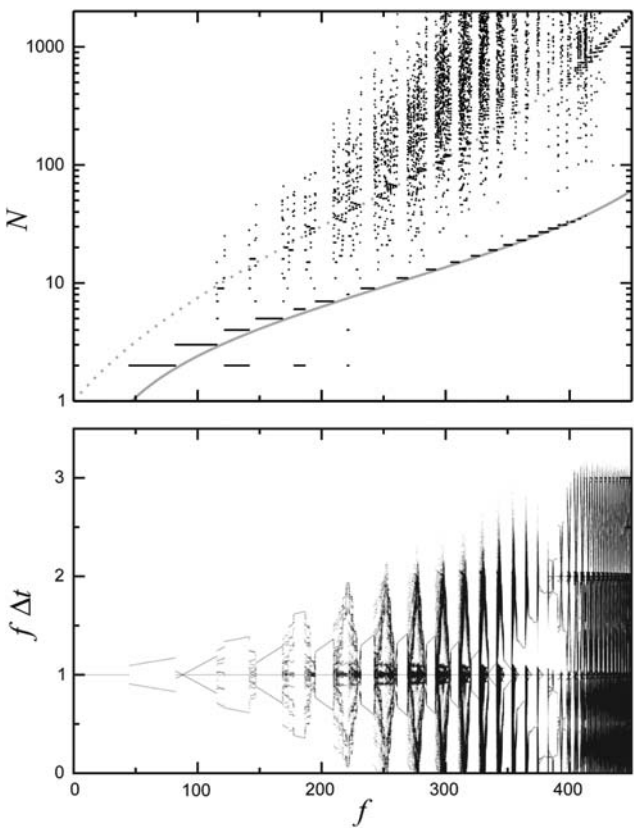

Fig. 6 Results from the asymmetric loop ($L_a = 2.1$ mm, $L_b = 2$ mm) for droplets of the equivalent length $\delta L_{\text{drop}} = 0.4$ mm for $f_{\infty\ \text{eff}} = 525.8$ Hz. Length of cycle, N (if periodic) and theoretically estimated number of droplets, n_{theo} (solid curve) are shown in the upper plot, whereas the lower plot shows normalized time intervals between subsequent droplets arriving at the outlet; both plots share the same axis of frequency, f.

As the ratio of r to the basic resistance of the channels $R_{0\ a/b}$ increases, the diagrams and maps of periodicity become more "discrete": the distance between neighboring regular areas, as well as their volume, become larger. In the map of the regular areas (Fig. 4.b) one can observe horizontal stripes divided by lines of discontinuous changes in the periodicity of the cycles. The width of these stripes (their range in the dimension spanned by L) is directly related (and equal) to the added resistance of the droplet (in simulations shown in Fig. 4.b r corresponded to $\delta L_{\mathrm{drop}} = 200$ μm).

Another (quantitative) effect of increasing r is the vanishing of odd periodicities in the symmetric loop. For r corresponding to $\delta L_{\mathrm{drop}} = 200$ μm we recorded that the largest odd period in the symmetric loop was $N = 11$. As r increases the maximum odd N in the regular regions of symmetric loop become smaller: for example, the region with $N = 5$ is unavailable for $\delta L_{\mathrm{drop}}/L_a > 0.28$.

Fig. 6 exemplifies also a generic difference between the dynamics in a symmetric and asymmetric loops. In the case of a symmetric loop (Fig. 3) all the subsequent even values of N form a regular staircase which become denser and denser up to the infinity, reached for $f_{\infty\ \mathrm{eff}}$. In the asymmetric loop there is no synchronization frequency and the series of "regular" bands is abrupted at a finite value of f. Also, the diagram of time intervals between consecutive outgoing droplets is different: the regular areas have three different intervals rather than one as in Fig. 3.b (in general, as the asymmetry increases, the diagram becomes more and more complicated - there can be up to N distinct intervals for a periodic trajectory with period N).

5.6 Constant pressure *versus* constant rate of flow

In this paper we restricted our description to systems driven at constant pressure with the rate of flow Q being dependant on p and on the distribution of droplets. We also performed similar analyses for systems with fixed Q and dependant p. Qualitatively, the results were similar; the main difference was the lack of critical frequency f_∞. As a consequence, bands of regular and irregular motion for the symmetric loop are evenly spaced along the f-axis.

6 Experiment

Below we describe the experimental results that recaptured the theoretical and numerical findings. In particular we were able to observe experimentally: (i) the existence of memory, (ii) same combinatorial composition of patterns for a given period of the cycle as predicted numerically, and (iii) the existence of regions of regular (cyclic) dynamics adjacent to bands of irregular behaviors.

6.1 Experimental setup

We fabricated the microfluidic device by direct milling (with a CNC milling machine MSG 4025, Ergwind, Poland) in polycarbonate (Macroclear, Bayer, Germany). The device was sealed by bonding with a flat slab of polycarbonate. The bonding process is preceded by a 15 min exposure of the pieces to vapors of 25%/75% (w/w) dichloromethane/isopropanol in a closed chamber at room temperature and atmospheric pressure. Then the pieces are bonded together under 130 °C in a press. The loop consisted of two nominally identical channels of 13 mm in length, connected in parallel (by T-junctions) between short input and output channels. All channels had square cross-sections of 200μm in width and height.

Droplets were formed at the beginning of the input channel by a cross-junction of channels of the same square profile. One of the key assumptions in our theory and simulations is that the process of generation of droplets is completely independent of the motion of the droplets already contained in the system; *i.e.* we assume constant frequency of emission of droplets into the system, independently of its state (*e.g.* resistance). In order to obtain an approximation of this condition in experiment we introduced large hydraulic resistances to connect the pressurized containers with the fluids to the microfluidic chip. We used steel capillaries of internal diameter of 200 μm and of length of 60 cm. The resistance of these capillaries was about 50 times larger than the resistance of the chip. This configuration ensures that the changes of the resistance of the chip (due to the varying distribution of droplets in the channels) do not affect the rate of flow of any of the two immiscible fluids appreciably. Further, on the line that fed the aqueous (droplet) phase we positioned a short elastic section and a "pressure pulser" made from a modified solenoid squeeze valve (Sirai, Z031A, Italy) that periodically generated short pulses of pressure by tapping on the elastic tubing. The internal clearance of the tubing was changed by the strokes of the valve. Setting the frequency of the valve close to the natural frequency of the system (*i.e.* with valve completely open) stabilized the frequency of formation of droplets. The limitation of this system was that it was difficult to change the frequency of formation of droplets without introduction of a simultaneous change of their volumes, which effectively prohibited us from performing extensive scans of the behavior of the system.

As the two immiscible liquids we used a 1% (w/w) solution of Span 80 (Sigma) in n-hexadecane (Reachim/Sojuzchimexport, USSR) and a 38/38/12/12 (w/w/w/w) mixture of purified water (Millipore), glycerol (Fluka), blue Parker Quink and black Waterman ink respectively; viscosities of both liquids at room temperature are in the range of 3 mPa s ± 10% (on the basis of data for pure hexadecane[27] and water-glycerol mixture[28]). As the driving pressure we used hydrostatic pressure difference. We mounted vertical steel rails and positioned the containers on linear translation stages (Thorlabs) that were attached to the rails with the help of magnets. Sliding the magnets on the rails and adjusting the position of the linear translation stages allowed for fine tuning of the pressures applied to the inlets. In order to introduce perturbations (to change a memorized pattern into another one), we changed parameters temporarily; the easiest way to do it was a rapid change in pressure caused by striking the elastic tubing used as the influx of oil or the aqueous phase (a typical result of such a perturbation is shown in Fig. 7.F.

6.2 Combinatorial composition of the patterns

Our experiments captured all of the salient features of the results of simulations. Our goal was to find all permitted sequences for a given number of droplets in the loop and to compare the findings with simulations. For example, we found all 10 possible patterns for $N = 8$ (movies with these patterns are available in

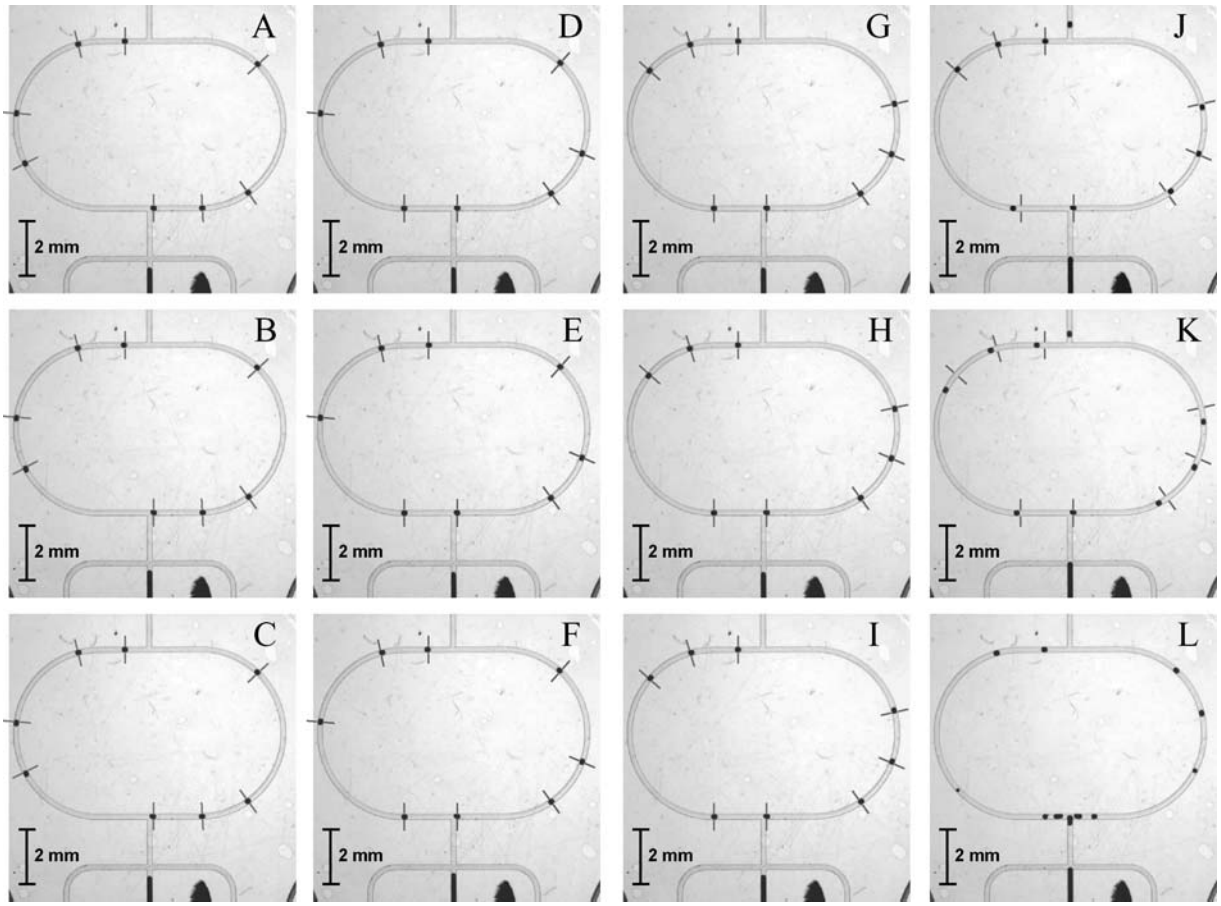

Fig. 7 Micrographs documenting the repeatability of the cyclic sequences of trajectories of droplets and the distribution of droplets in the two arms of a symmetric loop. In micrographs A–I the droplets were introduced into the loop at a frequency of $f \approx 1.5$ Hz. The three columns (containing pictures A–C, D–F, G–I) show three out of 10 possible stable cyclic sequences: LLRLLRRR, LLRLRRLR and LLLRRRLR respectively. In each of the columns, we mark the positions of the droplets in the first frame (the topmost micrograph) and copy these positions on the two bottom micrographs in each column. The two bottom micrographs were taken a number of periods after the first one: (B was taken 7 cycles after A, C 31 cycles after A; E 6 and F 26 after D; H 21 and I 40 after F). The different delays represented in the pictures result from the fact that we used a standard camera to record the images (at 14.09 frames per second) and we had to choose the images that matched the phase shown in the upper insets as close as possible. Insets J and K document the dynamics of the system in an irregular band at $f \approx 1.6$ Hz (see the text) and inset L shows system immediately after a deliberate 'disturbance' (a tap on the tubing feeding the aqueous phase) that we used to switch the system between different stable cyclic sequences.

Electronic Supplementary Information†) and all 4 patterns for $N = 6$ (as they were listed in sect.4.2). Also for N in range from 1 to 4 the behavior of the system was in complete agreement with the model (*e.g.* for $N = 4$ we observed sequences RRLL and RL, as the model predicts).

In experiments we did not observe any stable sequences with periods $N = 5$ or larger odd integers. The lack of such periods may be explained by the discussion in section 5.5: possibly in our experiments the resistance of a single droplet (expressed in the equivalent length of the channel δL_{drop}) was higher than 28% of the length of the single arm.

6.3 Regular and irregular bands of frequency

Using the droplet on demand system (with limitations described in section 6.1) driven by an electronic pulse generator we also confirmed the existence of regular and irregular bands of frequency, as it was predicted by our model. We set the rate of flow of the continuous phase to 200 nl s^{-1}, which corresponds to a linear velocity of droplets in a single arm of about 2.5 mm s^{-1} and the Reynolds number $Re \sim 0.2$. By changing the frequency of generation of droplets we were able to either maintain a memorized pattern (when the frequency was still within the regular band) or to move into a region of irregular dynamics where no stable patterns were observed. Even if a long-period pattern would be theoretically possible, the fluctuations of parameters make them experimentally unavailable.

In first three columns of Fig. 7 we show three—out of the total number of 10 recorded—stable sequences of period $N = 8$ obtained within a regular band at $f = 1.5$ Hz. For example, micrographs A to C show three snapshots of the sequence LLRLLRRR. The micrographs were recorded just after the last R in the sequence (*i.e.* when the droplet next to the input channel has just turned right), *i.e.* at multiplicities of the period of the system (equal to 5.333 s). The positions of the centers of the droplets in micrograph A are shown also in snapshots B and C. One can observe the striking reproducibility of the pattern. Analogous data for two other sequences (LLRLRRLR and

LLLRRRLR) are shown in insets D–F and G–I, respectively. All these patterns (and the remaining 7 shown in supplementary information) are stable: small perturbations are not amplified and in order to switch the system from one sequence (temporal pattern) to another one we needed to introduce a deliberate (and large) stimulus (as shown in inset L).

For a comparison, snapshots J and K show micrographs obtained in the irregular band: for $f = 1.6$ Hz. In this case the configuration of droplets does not form a repeatable pattern. The snapshot were taken when the fragments of the observed series of L/R choices resembled the pattern from the snapshot G (also the position markers in J and K are copied from G). Literally, the snapshot J was made at the last R in the fragment indicated by upper case letters in the following series:

[...]lrrrrlllrlrrrlllrrlrrlllrrrlrllrlrrrllllrl
rrrlrLLLRRRLRllrlrrlrllrlrrrllllrrlrrlrllrlrrlr
llrrlrlrllrrrllllrrlrrlrllrlrrlrllrrlrlrrl[...]

whereas for the snapshot K:

[...]rrrllllrrrrllllrlrrrllllrrlrrllrlrlrrrllllrr
lrrllllrrrlrllllrrrrllllllrrrrllllrlrrrllllrrlrrrllll
rlrrrllllrrlrrLLLRRRLRllrlrrlrlrllrrrllllrr[...]

Each time when we decreased f back to the stable band, one of the possible cyclic patterns emerged. We note that we were not able to obtain all 10 combinatorial patterns only by changing the frequency between 1.5 and 1.6 Hz. We found, however, that changes in r and rapid changes of p achieved by striking the tubing made it possible to obtain all 10 sequences predicted by combinatorial considerations.

We note the perfect qualitative and—in some aspects—quantitative agreement between the experiment and the numerical and theoretical predictions. We believe that a series of more detailed experiments could provide a fully quantitative agreement which would build a predictive tool for use in designing complicated chemical protocols to be performed in microfluidic networks of channels. Such a numerical model can be extended to comprise the more sophisticated details of the dynamics of real (physical) systems. These details could include (i) the effects introduced by the finite size of the droplets, (ii) delays introduced by the stagnation of the droplets at the junctions,[19,20,29] (iii) non-linear dependence of the rate of flow on the pressure drop along a channel, (iv) a dependence of the resistance introduced by a droplet on the speed of flow,[14,15,25] and (v) influence of the experimental imperfections on the times of emission and volumes of consecutive droplets.

7 Summary

We have demonstrated a detailed numerical and combinatorial analysis of the dynamics of the flow of droplets through the simplest microfluidic network – a single section of two parallel channels, and detailed the possible temporal patterns of flow of droplets through this system. Our analysis demonstrated the existence of regular regions with degenerate stable sequences of trajectories of droplets. This behavior exhibits microfluidic memory in that any particular sequence can be continued *ad infinitum* unless the system is switched to a different cyclic pattern.

The results are highly non trivial: we hope to have provided the basic insight into the mechanisms behind the observed regularity of the cycles on the example of a symmetric loop operated at synchronization frequencies. However, the cyclic behaviors persists also for frequencies that do not synchronize the events of entering and exiting the loop by consecutive droplets in a symmetric loop, and for asymmetric loops (in which there are no synchronization frequencies).

As we were able to recuperate all the salient features of the numerical and theoretical predictions in experiments we believe that the flow of droplets through microfluidic networks can be successfully modeled and that numerical schemes can be constructed to present high predictive power. This correspondance between theory and experiment may become usefull in designing automated micro laboratories capable to perfrom complex screens in analytical and synthetic chemistry.

Acknowledgement

Project operated within the Foundation for Polish Science Team Programme co-financed by the EU European Regional Development Fund and within the project **N20208831/0599** supported by the Polish Ministry of Science and Higher Education (2006–2009). P.G. acknowledges support from the Foundation for Polish Science under the Homing program.

References

1 T. Thorsen, R. W. Roberts, F. H. Arnold and S. R. Quake, *Phys. Rev. Lett.*, 2001, **86**, 4163–4166.
2 S. Anna, N. Bontoux and H. Stone, *Appl. Phys. Lett.*, 2003, **82**, 364–366.
3 P. Garstecki, M. Fuerstman, H. Stone and G. Whitesides, *Lab Chip*, 2006, **6**, 437–446.
4 A. Ganan-Calvo, *Phys. Rev. Lett.*, 1998, **80**, 285–288.
5 P. Garstecki, I. Gitlin, W. DiLuzio, G. Whitesides, E. Kumacheva and H. Stone, *Appl. Phys. Lett.*, 2004, **85**, 2649–2651.
6 H. Song, D. L. Chen and R. F. Ismagilov, *Angew. Chem., Int. Ed.*, 2006, **45**, 7336–7356.
7 P. Garstecki, H. Stone and G. Whitesides, *Phys. Rev. Lett.*, 2005, **94**, 164501.
8 B. Dollet, W. van Hoeve, J.-P. Raven, P. Marmottant and M. Versluis, *Phys. Rev. Lett.*, 2008, **100**, 034504.
9 A. Gunther and K. F. Jensen, *Lab Chip*, 2006, **6**, 1487–1503.
10 G. Cristobal, J. P. Benoit, M. Joanicot and A. Ajdari, *Appl. Phys. Lett.*, 2006, **89**, 034104.
11 F. Jousse, R. Farr, D. R. Link, M. J. Fuerstman and P. Garstecki, *Phys. Rev. E: Stat., Nonlinear, Soft Matter Phys.*, 2006, **74**, 036311.
12 M. J. Fuerstman, P. Garstecki and G. M. Whitesides, *Science*, 2007, **315**, 828–832.
13 M. Schindler and A. Ajdari, *Phys. Rev. Lett.*, 2008, **100**, 044501.
14 M. J. Fuerstman, A. Lai, M. E. Thurlow, S. S. Shevkoplyas, H. A. Stone and G. M. Whitesides, *Lab Chip*, 2007, **7**, 1479–1489.
15 V. Labrot, M. Schindler, P. Guillot, A. Colin and M. Joanicot, *Biomicrofluidics*, 2009, **3**, 012804.
16 M. Prakash and N. Gershenfeld, *Science*, 2007, **315**, 832–835.
17 G. F. Christopher, N. N. Noharuddin, J. A. Taylor and S. L. Anna, *Phys. Rev. E: Stat., Nonlinear, Soft Matter Phys.*, 2008, **78**, 036317.
18 W. Lee, L. M. Walker and S. L. Anna, *Phys. Fluids*, 2009, **21**, 032103.
19 D. Link, S. Anna, D. Weitz and H. Stone, *Phys. Rev. Lett.*, 2004, **92**, 054503.
20 G. F. Christopher, J. Bergstein, N. B. End, M. Poon, C. Nguyen and S. L. Anna, *Lab Chip*, 2009, **9**, 1102–1109.

21 M. Chabert, K. Dorfman and J. Viovy, *Electrophoresis*, 2005, **26**, 3706–3715.
22 D. Link, E. Grasland-Mongrain, A. Duri, F. Sarrazin, Z. Cheng, G. Cristobal, M. Marquez and D. Weitz, *Angew. Chem., Int. Ed.*, 2006, **45**, 2556–2560.
23 M. L. Cordero, D. R. Burnham, C. N. Baroud and D. McGloin, *Appl. Phys. Lett.*, 2008, **93**, 034107.
24 O. Cybulski, *SPICE'd Microfluidics*, 2007, presentation at Coding and Computation in Microfluidics, http://cba.mit.edu/events/07.05.fluid/.
25 S. A. Vanapalli, A. G. Banpurkar, D. van den Ende, M. H. G. Duits and F. Mugele, *Lab Chip*, 2009, **9**, 982–990.
26 A. Davis, *Gnucap – Gnu Circuit Analysis Package*, http://www.gnucap.org/.
27 C. Wohlfarth, *Landolt-Boernstein, New Series, IV/25 (Supplement to IV/18), Viscosity of hexadecane*, Springer, 2009, pp. 655–656.
28 *Viscosity of Aqueous Glycerine Solutions* (*Dow*, *Optim Glycerine*), http://www.dow.com/glycerine/resources/table18.htm.
29 M. De Menech, *Phys. Rev. E: Stat., Nonlinear, Soft Matter Phys.*, 2006, **73**, 031505.